INTEGRATING SPATIAL REASONING INTO NEURAL GENERATIVE MODELS FOR DESIGN PRODUCTION

A PREPRINT

Maxwell J. Jacobson
Purdue University
Department of Computer Science, USA
jacobs57@purdue.edu

Yexiang Xue
Purdue University
Department of Computer Science, USA
yexiang@purdue.edu

ABSTRACT

Good designs must meet explicit user needs and honor implicit rules related to aesthetics, utility, and convenience. Current automated design tools driven by machine learning alone produce appealing designs but cannot satisfy user specifications and utility requirements. Constraint reasoning tools alone cannot produce design visualizations. We introduce Spatial Reasoning Integrated Generator (SPRING) for design production. SPRING embeds a spatial reasoning module inside the generative neural network. The spatial reasoning module decides the locations of the objects to be generated in the form of bounding boxes predicted by a recurrent network-driven iterative refinement approach filtered by constraint satisfaction. Embedding constraint reasoning into learning guarantees the output of SPRING satisfies user requirements. Furthermore, SPRING offers interpretability, allowing users to visualize and diagnose the generation process through the bounding boxes. SPRING also handles novel user specifications not present in the training set well in the zero-shot transfer learning setting. Our experiments, backed by a human study, demonstrate that SPRING surpasses baseline generative models by delivering high image quality and superior satisfaction in meeting user specifications.

Keywords Constraint Reasoning, Spatial Reasoning, Neural Generative Models, Constrained Content Generation

1 Introduction

A good design needs to meet industry standards and user needs, while at the same time capturing subtle aspects such as aesthetics and convenience. A constraint program can be defined to find a plan which meets all standards and needs, but constraint programs cannot provide visualizations of the designs. Moreover, the designs generated by constraint programming often satisfy the bare minimum of functionality without considering subtle aspects. In fact, it is almost impossible to encode aesthetics into the objective function of a constraint program. Hence, the designs solely generated by constraint satisfaction are often not welcomed by customers. Recent advancements in machine learning, particularly in deep generative models, have presented new opportunities for addressing these challenges. Text-to-image and graph-to-image models provide exciting possibilities for controllable generation, but their control is not always precise enough to produce designs that meet complex specifications. For example, in Figure 1, a toaster must be added to the left of the oven and below the sink, and a microwave needs to be added to the right of the oven. In the right panel, the Stable Diffusion model taking the input of the initial kitchen configuration and the text specifications simply alters the entire scene. Overall, AI-driven automatic design is an emerging field that requires *the integration of machine learning and constraint reasoning*. However, such integration is beyond the reach of state-of-the-art models.

Our Approach. We introduce **Sp**atial **R**easoning **In**tegrated **G**enerator (SPRING) for design production. Given an initial indoor scene and user requirements described in propositional logic, the task is to generate a design that satisfies user specifications, looks pleasing and follows common sense. The essence of SPRING is the *embedding of a spatial reasoning module inside the deep generative network*. The spatial reasoning module decides the locations of the objects to be generated in the form of bounding boxes following an iterative refinement approach. The bounding boxes are predicted by Recurrent Neural Networks (RNNs) and are further filtered by constraint reasoning (forward checking).

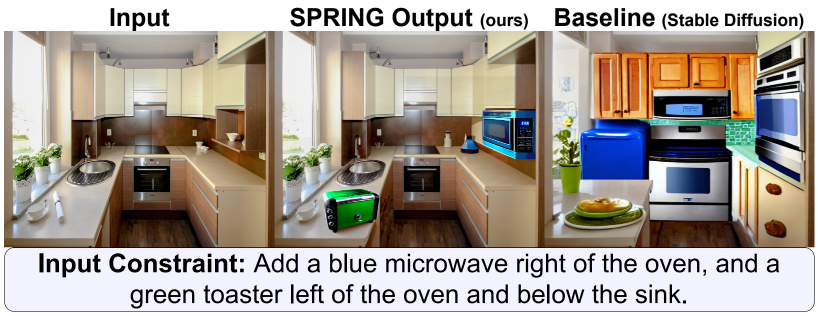

Figure 1: An interior design generated by SPRING (middle) with a given background already containing an oven and a sink among other objects (left). The user specifications are at the bottom (provided to SPRING in the form of propositional logic; natural language text is used here to aid readability). SPRING creates a design satisfying the specifications. Text-to-image approaches like Stable Diffusion (right) often fail to meet these constraints.

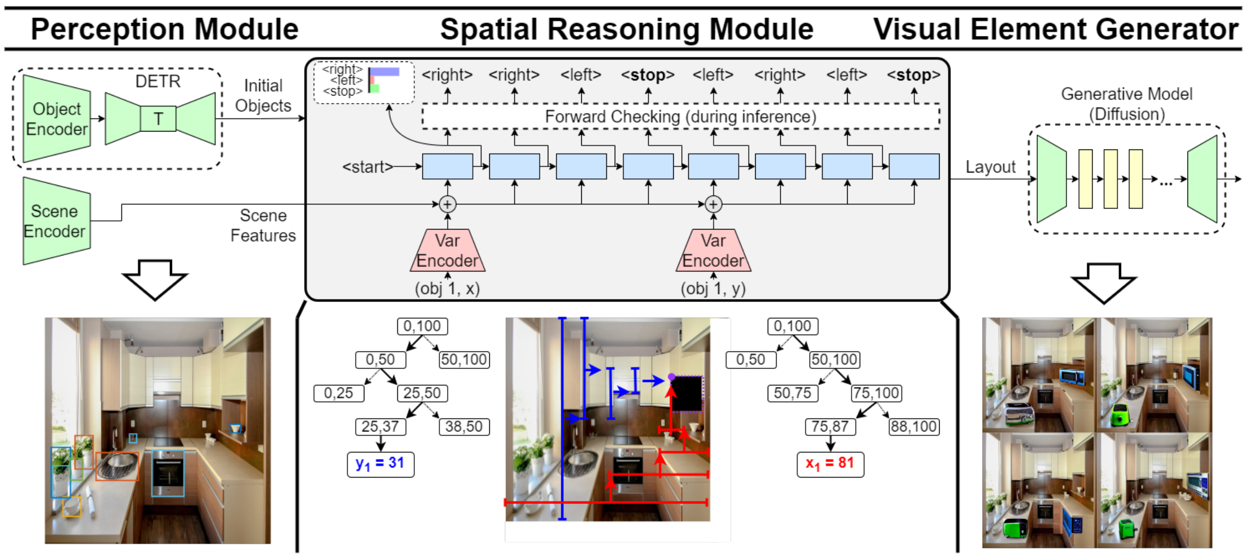

Figure 2: Rollout of the SPRING system. The top shows the architecture. The bottom shows the state of the image as it moves through the network. **(Left)** The perception module scans the initial image to extract existing objects (types and bounding boxes) and scene latent features. **(Center)** The spatial reasoning module takes as input the scene features, the set of initial objects, and the user-defined specification for new objects. It outputs a layout for the image with all positional variables (*x, y, width, height*) decided for each object. The spatial reasoning module is a GRU that outputs the coordinate of each object sequentially. The value of each coordinate is narrowed down via *iterative refinement* until the stop token is selected. Constraint reasoning in the form of forward checking is applied during inference which filters out coordinate assignments that violate user specifications. The decision-making process is visualized as a tree of value ranges to generate the x and y positions of the microwave. **(Right)** The visual element generator in the form of a diffusion model paints each object into the scene to produce the final image.

This integrated approach allows us to leverage the advantages of both approaches. Constraint satisfaction deals with explicit specifications, such as user requirements, while neural networks handle aesthetics and common sense.

SPRING consists of three modules. The first perception module based on Detection Transformers (DETR) [13] extracts existing object positions from input images. It is followed by the spatial reasoning module, which uses constraint reasoning integrated learning to generate the bounding boxes. When determining one coordinate variable of the bounding box, the RNN in the spatial reasoning module iteratively halves the range of the coordinate until it is sufficiently small. During learning, the RNN is trained to understand implicit spatial knowledge, such as potted plants usually being located on the floor, etc. This is completed by a teacher-forcing procedure that matches the bounding boxes predicted by the RNN and the ones containing the objects in the training image. During inference, explicit spatial constraints are enforced by a forward-checking algorithm, which blocks the decisions leading to constraint violations. Finally, the bounding boxes are filled by the third visual element generator module, which is a diffusion model. The three modules of SPRING are illustrated in Figure 2.

How SPRING Advances the State-of-the-art: *(1) Guaranteed User Requirement Satisfaction via Embedding Spatial Reasoning into Design Generation.* SPRING guarantees the generated designs satisfy user specifications. Learning to satisfy constraints in generative models is notoriously difficult. This is due to the intricate nature of constraint satisfaction, which is beyond the capabilities of current neural network approaches. It is also unnecessary for neural networks re-learn the meaning of specifications (such as the meaning of "to the left of"). Prior work [33] also generates bounding boxes in the process of image generation. The key difference between this work and our SPRING is that they used black-box graph neural networks for bounding box generation. As a result, they need to learn the meaning of constraints and do not have guaranteed performance. In the experiments, we show their models cannot produce designs with desired properties.

(2) Interpretable Model. SPRING is more interpretable than alternate methods. At each step of iterative refinement, the user can view the probabilities associated with each sub-decision while also tracing the path of the forward-checker to see constraint violations. Users can follow this trace to diagnose the designs generated by SPRING.

(3) Zero-shot Transfer to Novel User Specifications. The forward-checking procedure also allows us to handle constraints in a zero-shot manner. When novel constraints not present in the training set are given at test time, the forward checking procedure still blocks the output of the RNNs in the same way as handling familiar constraints, without the need for any retraining or fine-tuning. This is demonstrated in Appendix C.

Evaluation. We evaluate SPRING in the domain of interior design visualization, in which the AI must add elements to an interior space like a kitchen or a living room, taking into account existing objects and constraints given by the user. The images produced by SPRING are on-par in quality with the latest image generation tools. This is verified from both visual inspection and quantitative scores. However, SPRING is able to produce designs that satisfy complex user specifications, while baseline approaches cannot. We also demonstrate that the designs generated by SPRING satisfy implicit spatial constraints, such as toasters should not be put on the floor, etc. Furthermore, SPRING is capable of handling novel user constraints not presented in the training set in the zero-shot learning setting, as evidenced by the implementation of a novel constraint after training was already complete. To complement these evaluations, we conducted a human study to assess the algorithm's performance in producing realistic images and satisfying user constraints. The results corroborate the effectiveness of SPRING in generating high-quality images that adhere to user specifications while maintaining the overall aesthetics and spatial naturalness of the design.

2 Problem Definition

Design production is the problem of producing designs in the form of diagrams, environments, or images. The example chiefly explored here is interior design, in which the image is an interior in a home, such as a kitchen or living room, and the design is specified as a set of objects to add which have positional relationships to each other and objects already in the image. The problem can be defined as:

Problem 1: *(Design Production):* ***Given:*** *let B be a background image that contains initial objects W, and D be a design specification with new objects O and positional constraints C represented in the propositional design language defined below. C may reference objects in both O and W. T is the set of "natural" images.*
Find *a scene image S, with B as a background, containing objects defined by O, such that all of C is satisfied and S is "realistic"; i.e., it is visually close to the images in T.*

2.1 Propositional Design Language

Symbols and Constants. Our design language uses propositional logic. In this language, $o_1, o_2, \ldots, o_N$ denote objects. These objects represent furniture or other objects that are either in the background image or need to be added. The constants used in the design language are integers and text strings. The integers are often used to denote the spatial distances between objects while text strings define the properties and types of the objects.

Properties and Types. `Property` is a predicate that evaluates to true if and only if an object has a given property. For example, $\texttt{property}(o_1, \text{“}blue''\text{)}$ is true if and only if object o_1 has the property “$blue''$ (i.e., its color is blue). A special property is called `type`. This defines the type of object being reasoned over from a set of known types. For example, $\texttt{type}(o_1, \text{“}microwave''\text{)}$ evaluates to true if and only if o_1 has the type “$microwave''$. Combining with the previous example, $\texttt{type}(o_1, \text{“}microwave''\text{)} \wedge \texttt{property}(o_1, \text{“}blue''\text{)}$ means object o_1 is a blue microwave. Our language recognizes the following types: chair, couch, potted plant, bed, mirror, dining table, window, desk, toilet, door, tv, microwave, oven, toaster, sink, refrigerator, and blender.

Relation	Truth condition
above(o_1, o_2, c)	the top side of o_1 is at least c units above the top side of o_2.
cabove(o_1, o_2)	the bottom side of o_1 is at least c units above the top side of o_2.
above_value(o_1, c)	the top side of o_1 has a y-value less than c.
below(o_1, o_2, c)	the top side of o_1 is at least c units below the top side of o_2.
cbelow(o_1, o_2)	the top side of o_1 is at least c units below the bottom side of o_2.
below_value(o_1, c)	the top side of o_1 has a y-value greater than c.
left(o_1, o_2, c)	the left side of o_1 is at least c units to the left of the left side of o_2.
cleft(o_1, o_2, c)	the right side of o_1 is at least c units to the left of the left side of o_2.
left_value(o_1, c)	the left side of o_1 has an x-value less than c.
right(o_1, o_2, c)	the left side of o_1 is at least c units to the right of the left side of o_2.
cright(o_1, o_2)	the left side of o_1 is at least c units to the right of the right side of o_2.
right_value(o_1, c)	the left side of o_1 has an x-value greater than c.
narrower(o_1, o_2, c)	object o_1 is at least c units narrower than object o_2.
narrower_value(o_1, c)	object o_1 has a width less than c.
shorter(o_1, o_2, c)	object o_1 is at least c units shorter than object o_2.
shorter_value(o_1, c)	object o_1 has a height less than c.
taller(o_1, o_2, c)	object o_1 is at least c units taller than object o_2.
taller_value(o_1, c)	object o_1 has a height greater than c.
wider(o_1, o_2, c)	object o_1 is at least c units wider than object o_2.
wider_value(o_1, c)	object o_1 has a width greater than c.
heq(o_1, o_2)	object o_1 and object o_2 have the same height.
heq_value(o_1, c)	object o_1 has a height equal to c.
weq(o_1, o_2)	object o_1 and object o_2 have the same width.
weq_value(o_1, c)	object o_1 has a width equal to c.
xeq(o_1, o_2)	the left side of o_1 is in line with the left side of o_2.
xeq_value(o_1, c)	the left side of o_1 has an x-value equal to c.
yeq(o_1, o_2)	the top side of o_1 is in line with the top side of o_2.
yeq_value(o_1, c)	the top side of o_1 has a y-value equal to c.

Table 1: Spatial relations and their truth conditions. Note that integer literals (shown here as c) are in units of per-thousanths of the background image's width and height.

Relations. Relations are used to model spatial constraints between objects, providing a way to describe the relative position, size, and alignment of objects within a design. These relations evaluate to true if the spatial relationship is upheld between the objects included, and false otherwise. Our grammar includes various types of predicates to express these relationships.

1. **Spatial relationships with constant offsets:** This group of predicates defines spatial relationships between two objects with a constant offset. Predicates like `above`, `below`, `right`, and `left` describe relative positions between objects in the x and y dimensions. For example, $\texttt{above}(o_1, o_2, k)$ is true if and only if object o_1 is above object o_2 by k vertical units. More precisely, the top side of o_1 is at least k vertical units above the top side of o_2. In this paper, one vertical (horizontal) unit is measured as one-thousandth of the height (width) of the image. Sometimes the distance k is omitted. In this case, $\texttt{above}(o_1, o_2)$ is true if and only if o_1 is above o_2. Additionally, the grammar provides `cabove`, `cbelow`, `cright`, and `cleft` predicates, which represent complete spatial constraints where the entire bounding box of one object is constrained in one direction away from its counterpart, with no overlap. For example, $\texttt{cabove}(o_1, o_2, k)$ holds if and only if object o_1 is completely above object o_2 with a constant vertical distance of at least k. In other words, the bottom side of o_1 is at least c vertical units above the top side of o_2.

2. **Size comparisons between objects:** `shorter`, `taller`, `narrower`, and `wider` predicates define the size constraints between objects. For example, $\texttt{shorter}(o_1, o_2, c)$ evaluates to true if and only if object o_1 is at least c vertical units shorter than object o_2. Again, the argument c can be omitted.

3. **Equality constraints:** These predicates establish equal attribute relationships between objects. For example, $\texttt{xeq}(o_1, o_2)$ holds if and only if objects o_1 and o_2 share the same x-position (meaning they are vertically aligned). Similarly, `yeq`, `weq`, and `heq` predicates ensure that two objects share the same y-position, width, or height, respectively.

4. **Constraints with constant values:** This group of predicates sets specific constraints on an object's attribute with a constant value instead of in reference to another object. For example, above_value(o, k) holds if and only if the y-position of the top-left corner of object o is above (less than) k. Similarly, other predicates like below_value, right_value, left_value, shorter_value, taller_value, narrower_value, wider_value, xeq_value, yeq_value, weq_value, and heq_value constrain an object based on given values.

Complex Relationship. The complex spatial relationship among objects can be defined using logic operators ($\wedge$ for "and", $\vee$ for "or", $\neg$ for "not") to connect the set of predicates discussed above. For example, "a cozy brown leather chair is either completely left or completely right of the black and white striped couch." can be described as:

$$\begin{aligned}&\texttt{type}(o_1, \text{“}chair'') \wedge \texttt{property}(o_1, \text{“}cozy'') \wedge \texttt{property}(o_1, \text{“}brown'')\wedge\\&\texttt{type}(o_2, \text{“}couch'') \wedge \texttt{property}(o_2, \text{“}black\ and\ white\ striped'')\wedge\\&(\texttt{cleft}(o_1, o_2) \vee \texttt{cright}(o_1, o_2)).\end{aligned}$$

This completes our definition of the propositional design language. While natural language is usually easier to use than structured languages like ours, it may suffer from ambiguities, which render it difficult to satisfy hard rules. Nevertheless, we intend to eventually extend our work to consider natural language as well. We leave such effort for future work.

3 Spatial Reasoning Integrated Generator

SPRING is motivated by the desire to smoothly integrate the handling of implicit preferences from data and explicit rules from the user to generate high quality design images. SPRING is composed of a perception module, a spatial reasoning module, and a visual element generation module.

The ***perception module*** serves to extract the types and positions of objects already existing in the background image. The ***spatial reasoning module*** decides the spatial position of each object. In our setting, the spatial position is represented as a bounding box with parameters (*x, y, width, height*). Here, *x, y* is the coordinate of the upper-left corner and *width, height* represent the width and height of the bounding box. We generate the bounding boxes of each object following an *iterative refinement* process, integrating neural network prediction and constraint reasoning. In particular, a recursive neural network based on GRUs [17] iteratively halves the range of each coordinate. For example, the range of x starts at the width of the image. In one step, GRU decides whether we should halve the range of x to be the left side or the right side. Such steps repeat until the range of x is sufficiently small and the middle point is chosen. During this process, a forward-checking algorithm rules out invalid outputs which violate user specifications. Note that the forward-checking algorithm fits seamlessly with the GRU, does not need to be trained, and can be edited programmatically without affecting the operation of the GRU. The decisions made by the GRU take into account both implicit preferences and explicit rules. During learning, the spatial reasoning module is presented with a set of background images and the corresponding bounding boxes of various objects in the images and is trained to predict the boxes that match those in the training set. In this way, GRU learns to meet implicit preferences such as "chairs don't float in the sky". The constraint reasoning tool (forward-checking) embedded in the spatial reasoning module allows SPRING to be transferred to new constraints not presented in the training set in a zero-shot learning setting. In the third step, the ***visual element generation module*** takes as input the background, the prompt, and location of each object in the form of a layout, and outputs an image patch which contains the object and can be merged seamlessly into the background image.

3.1 Perception Module

The purpose of the perception module is to extract information about the existing background for the SRM – which is utilized both in iterative refinement for implicit preference decision-making and forward checking for explicit rule decision-making. The perception module includes an object detector for existing object prediction and a scene encoder for scene-level feature extraction. The object detector is implemented with a pre-trained DETR50 [13] object-detection model trained on the COCO dataset [41], but this can be jointly trained with the spatial reasoning module given a new dataset. This part of the module predicts the types and locations of existing objects with a reported average precision of 42.0% on the COCO 2017 validation set. This is deemed sufficient for this work, particularly because the user-input step occurs after scanning, so these predictions can be verified by a human at this time. The objects predicted are encoded into the SRM hidden state through a deterministic forward pass, but they can also be referenced in the propositional logic constraint language. A Resnet18 [28] architecture pre-trained on ImageNet [19] is used as the scene encoder, which is fine-tuned during training as a part of the SRM. The features it encodes are used to instantiate the hidden state of the SRM, which is updated by that module's variable encoders and the main GRU itself.

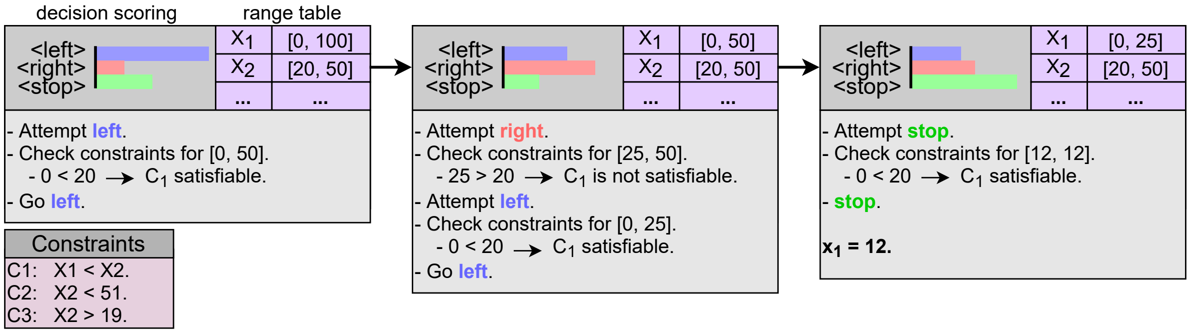

Figure 3: Example of forward checking in the SRM. In each step, a decision is sampled based on the probability distribution predicted by the GRU. A forward-checking procedure checks if the sampled decision leads to constraint violations. If it leads to, new decisions are sampled from remaining actions until no constraint violations. This process repeats in generating each decision.

3.2 Spatial Reasoning Module (SRM)

Architecture & Semantics of the SRM. In our setting, the spatial position is represented as a bounding box with parameters (*x, y, width, height*). Here, *x, y* is the coordinate of the upper-left corner and *width, height* represent the width and height of the bounding box. The set of these bounding boxes is conventionally known as a "layout" [74]. The spatial reasoning module takes the input of the background image as well as object identifiers, and outputs a layout. We use encoder networks to encode both the background image and the object identifier (e.g., object 0, type "chair") into high-dimensional vectors. The spatial reasoning module harnesses a Recurrent Neural Net (RNN) structure and outputs the four coordinates sequentially. This means the SRM draws from the background image, the current object type, and all previous decisions to produce its next decision in the sequence. Existing objects and their positions from the perception module are also fed into the network and deterministically to encode them into the hidden state.

The key idea in generating each coordinate is through *iterative refinement*. The basic unit of the RNN output is the *decision token* – a size 4 vector representing a score distribution of three possible decisions and one special start token. The input at each timestep is the previous timestep's decision as a one-hot vector. The network outputs at each step a softmax vector to assign the probability to each token. At the start of calculation, the selected variable is presumed to be within a given range (e.g. the first object's *x* value is between 0 and 100). The actions are to limit the position to be in the first half of the range (e.g. left: $0 \leq x < 50$), or in the second half of the range (e.g. right: $50 < x \leq 100$), or to terminate and select the middle value between the current minimum and maximum as the final location (e.g. stop: $x = 50$). This produces a *sequence of decisions* leading to the assignment to the corresponding variable. The sequence is embodied as a *decision string* composed of *decision tokens*. For example, the variable *x* between 0 and 100 may be assigned the decision string "left, right, stop", refining the value to $0 \leq x < 50$ as we choose the left of the range, then $25 < x < 50$ as we choose the right of the range, then $x = 37$ as we choose the center of the range. Our recurrent neural network is implemented in the form of GRUs. All contextual data including the background image encoding and the variable encoding is introduced into the GRU state vector (size 500) by adding to it. Figure 2 shows the processes of generating two coordinates x_1 and y_1 using the proposed neural network module, including the encoding at the start of each variable. See Appendix D for more on our architecture and hyperparameters.

Forward-checking in the SRM. The SRM's GRU network outputs a decision string for each positional variable by sampling tokens from the probability distribution output from the iterative refinement process until a conclusive value is reached. At the beginning of a string, the start token is given as input and the variable encoder adds information to the GRU state vector. The decisions are sampled based on the probabilities output by the spatial reasoning module. For example, if the module outputs the scores $[left : 75\%, right : 5\%, stop : 20\%]$, the spatial reasoning module will select "left" 75% of the time, "right" 5% of the time, and will choose to stop 20% of the time and to choose the middle value of the current range.

Forward checking is then used to explicitly enforce positional constraints from the users. They can be enforced by limiting the decisions considered in the sampling process – ensuring that decisions which lead to constraints violation are ignored. For each decision in the iterative refinement, the algorithm checks that the current value range contains at least one value assignment which satisfies all constraints. If at least one constraint must be violated, the SRM rewinds the decision string one token and resamples without the option of the original choice. Our forward checking algorithm is implemented as a depth first search exploring all future expansions of the decision strings – though many algorithms could fit this role. This forward checking process is conducted after each decision made by the GRU to see if constraint satisfaction is still possible. In our previous example, we may have selected the "left" token first, but then found that no value in the remaining range for that variable can satisfy all the constraints. We resample this token with new scores $[left : 0\%, right : 20\%, stop : 80\%]$. Given this recalculation, the stop token is now the most likely to be chosen. The process is visualized in Figure 3.

Learning the SRM. Aside from the explicit constraints given by the users, the locations predicted by the SRM should satisfy implicit preferences such as "toasters are rarely placed on the ground". The training of SRM uses a dataset containing background images with a bounding box for each object to be generated. Each object's location is defined by the upper left point, as well as the width and height of the bounding box. These variables are converted to decision strings as described in the previous sections. The training process is a supervised procedure – it trains the spatial reasoning module to generate bounding boxes (in the form of decision strings) which match those in the training dataset. This procedure teaches the neural network implicit spatial knowledge including the relative sizes of objects and their common spatial relationships (toasters go on the counter, televisions might be hung on the wall, etc). We do not enforce explicit constraints during the training phase. The spatial reasoning module also needs to learn to encode the background image – extracting important features like the positions of the floor, ceiling, and walls. This is accomplished by the scene encoder in the perception module. Gradients are back-propagated through the scene encoder network as a unified model. More information on training can be found in Appendix D. The object detector portion of the perception module was not utilized during training, as all known existing objects were removed from training set backgrounds. However, SRM utilizes object-level information when generating designs, as explained in the next paragraph.

During design generation, existing objects perceived in the background image may influence the decisions made by the SRM. Not only should the user be able to set positional constraints that reference existing objects, but these objects must be encoded in the neural component of the SRM as well. This is done by making no distinction between objects that already exist in the background – those predicted by the perception module – and objects that need to be generated in the scope of the SRM. Each of the existing objects is constrained to their already-known positional values, but they are still processed through the SRM to update the hidden state. These are processed through the SRM first before new objects.

3.3 Visual Element Generator (VEG)

The bounding boxes from the spatial reasoning module let us generate each object into the scene using the visual element generator. The result is a completed scene adhering to the design with all positional constraints guaranteed. The visual element generation module is sequentially called on each bounding box created by the spatial reasoning module. We employ state-of-the-art neural generative models for the visual element generation module. Rather than training our own module, which would necessitate large datasets and significant effort, we opt to adapt and utilize existing cutting-edge neural models for greater efficiency and adaptability. Our implementation is capable of using either the reduced and filtered GLIDE [48] diffusion model released by OpenAI or the popular Stable Diffusion model [54] – more information on the configuration of these models is available in Appendix D. Given a masked image and a prompt, these networks inpaint the masked areas accordingly. One challenge of any diffusion model is the rare chance that it will generate the wrong object or no object at all. These inpainting failures are possible, though our method reduces them as each call is only responsible for a single object placed in a "good" location. Even so, objects that are painted correctly are guaranteed to follow positional constraints.

4 Related Work

Fast & Slow Thinking. Our work draws inspiration from the fast and slow thinking model described in works from cognitive psychology. Psychophysiological studies have long supported the concept of dual-process thinking in humans [59, 42] – in which more deliberate and more intuitive thinking are the result of separate fundamental processes. System 1 refers to a set of innate and learned automatic processes that are rapid, parallel, and unconscious. System 2 is responsible for abstract and hypothetical thinking and is slower, more deliberate, and more conscious [34, 24]. These concepts hold exciting parallels for the world of AI, which are already being seriously explored [39, 4, 10]. Our SPRING leverages neural networks for S1 cognition while delegating S2 cognition and planning to constraint reasoning. In this regard, our work takes inspiration from concepts like *fast and slow planning* [25], with the notable change that our system does not utilize any sort of meta-cognition AI-subsystem [26] to regulate between fast and slow thinking modules explicitly.

Constraint Reasoning & Machine Learning. The integration of constraint reasoning with machine learning has been a critical aspect of AI research, particularly in the context of deep learning. This integration aims to enhance reasoning capabilities and improve the performance of learning algorithms. Notable efforts in this domain include incorporating

Scenario	SPRING ⋆ Pref. Acc. ↑	Constr. Acc. ↑	GAN+CVX Pref. Acc. ↑	Constr. Acc. ↑
“Basic”	**1.0**	1.0	1.0	1.0
“Tight”	**0.917**	1.0	0.813	1.0
“Complex”	**0.875**	1.0	0.723	1.0

Table 2: Results for evaluating “goodness” of location decisions by the SRM when tested on synthetic scenarios. Our SPRING is able to generate object locations better satisfying implicit preferences from data (measured by preference accuracy) compared to baselines, while both approaches 100% satisfy constraints. Note, SPRING can also handle non-convex constraints, while “GAN+CVX” cannot. More details of this experiment are in Appendix E.2. ⋆ indicates our method.

Method	Position Acc. ↑	Object Acc. ↑	IS ↑	FID ↓
Stable Diffusion	0.5	0.63	3.58	162.73
sg2im	0.0	0.0	2.52	NaN
SPRING[SD] ⋆	**1.0**	**0.77**	**3.59**	**160.36**

Table 3: Abbreviated quantitative results from 10,000 generated scenes show our SPRING leads in position and object accuracy as well as Inception Score (IS) and Fréchet Inception Distance (FID) perception scores for visual image quality. FID statistics were calculated from the COCO 2017 validation set. Position accuracy represents how often the positional constraints are met. Object accuracy represents how often the correct number and type of objects are generated and identifiable. An extended table containing more baselines can be found in Appendix B.

"common-sense" reasoning into natural language models [29, 62, 49], case-based reasoning from expert systems [31], and relational reasoning between objects or terms [57, 38, 50, 72, 22].

Embedded constraint reasoning in machine learning is a promising idea [11, 66, 44, 9, 55], providing a structured way to incorporate domain knowledge and improve problem-solving capabilities. Convex optimization has been successfully employed as a neural net layer [12, 1, 3, 2], and other constraint reasoning methods have been integrated into neural nets for various applications [7, 20, 70, 5, 36, 15, 45]. Often, this integration comes in the form of using data to produce constraint models. Constraint acquisition enables learning of constraint networks from examples [8, 51, 63]. Other research investigates the reverse direction, where constraint models are embedded into networks to generate data. For example, decision diagrams have been successfully integrated into GANs for the purpose of constrained schedule generation [70], and similar approaches have excelled in other structured prediction tasks such as if-then program synthesis, text2SQL generation, and vehicle dispatch service planning [32].

Automatic Design. For the reasons previously discussed (addressing user needs and implicit conventions) most design domains have presented an exciting challenge for AI developers – recent progress has been made in architecture design [71], computer chip design [35], and biosystems [65]. Automatic interior design problems have been tackled in several ways previously [16] – including reinforcement learning [67] and conditional image generation [14]. Often, the data generated for this task is an abstract diagram of an interior space [37, 46, 47], but this approach is hard to visualize for a user. Other works focus on assisting the interior design process through images like ours [40], offering better visual qualities but less structure within the data itself. The most exciting methods are text-to-image and graph-to-image methods, which illustrate the possibilities and challenges of the domain.

Text-to-Image & Graph-to-Image Methods. Large diffusion models like DALL-E [53, 52], GLIDE [48], and Stable Diffusion [54] have been attracting attention as they can inpaint objects into scenes given a natural language prompt. These models have been made possible by large online datasets and the combination of transformer [64] and diffusion [58] technologies. However, they can fail on complex instructions, such as constraining the number and spatial relationships of objects. Recently, a line of research encodes requirements (such as image contents) into hidden vectors via graph or recurrent nets [18, 69, 23, 43], and then conditions image generation on these hidden vectors. This includes sg2im [33], which encodes positional relationships into scene graphs for image generation. However, it struggles with complex constraints and those not present in training. Other works [73, 21, 27] adapt this approach for image-to-image problems, using scene graphs as editable latent representations. Also related are layout-to-image approaches [74, 60] which generate an image from a background and a user-supplied layout, but they require the position of all objects to be strictly and completely defined by the user.

5 Experiments

Evaluating the performance of SPRING for interior design production involves examining three important aspects of the algorithm: the accuracy of the Spatial Reasoning Module’s spatial predictions, the ability to consistently meet design

Figure 4: Example visualizations from SPRING. Constraints are described in text for clarity. They were provided to SPRING in propositional logic (See Appendix A for logic definitions).

Method	Specification Satisfaction ↑	Aesthetics ↑	Background Preservation ↑	Spatial Naturalness ↑
SPRING	**4.068**	3.367	**4.473**	3.663
Stable Diffusion	2.240	**3.588**	2.608	**3.876**

Table 4: Results for the human survey with two methods: Stable Diffusion and SPRING (ours). Metrics collected include Likert scores (1-5) for specification satisfaction, aesthetic appeal, background preservation, and the naturalness of spatial qualities – e.g. proportions between objects, proportions between an object and the background. SPRING does much better at satisfying user specifications than Stable Diffusion, and is far less likely to damage the background due to its more controlled inpainting. SPRING receives slightly lower results for aesthetics and naturalness, perhaps representing a small trade-off between the amount of control provided by the algorithm and its ability to produce good-looking images.

requirements (i.e., constraints), and the realism of the final images produced by SPRING. It is important to emphasize that assessing the quality of generated images is a challenging problem in the field, and determining the naturalness of positions and dimensions, independent of aesthetic quality, is even more difficult. To tackle these challenges, the first aspect is evaluated using synthetic data scenarios for precise measurement, while the second and third aspects can be examined using real data and generated backgrounds. In order to address the known issues with more automatic metrics commonly employed in image generation tasks, a human survey was conducted, providing valuable insights into the overall performance of the SPRING algorithm. For all experiments, SPRING was trained on a subset of the COCO 2017 Detection dataset relating to interior design. It is difficult to find real-world datasets of background images (containing few objects) with bounding boxes of the objects to be generated. We instead use datasets of images containing objects

Figure 5: Comparisons between SPRING (VEG choice in brackets) and baselines on kitchen backgrounds. SPRING creates distinct objects and always follows positional constraints. Baseline methods produce compelling images, but rarely fulfill all constraints. They also greatly disrupt the background. Notice how the word "blue" affects the SPRING and baseline images. SPRING applies blueness to the microwave, while Stable Diffusion and GLIDE apply it to other parts of the image.

and their corresponding bounding boxes (such as COCO). We remove these objects from the original images using the Telea method [61]. This lets us train SPRING to place bounding boxes in their most natural positions. This step is discussed more in Appendix A.2.

5.1 Evaluating Image Quality

Setup. To evaluate the visual quality of the produced images, 10,000 scenes were generated from SPRING and from baselines using random specifications (see Appendix A.1). These specifications had no constraints on placement position. SPRING's performance was compared with Stable Diffusion, and SG2IM, representing text-to-image and graph-to-image methods, respectively. Another text-to-image baseline – GLIDE – was also compared in extended testing, which can be found in Appendix B. We employed natural language constraints to inpaint images using Stable Diffusion and programmatically constructed prompts derived from the same logic as SPRING. Rectangular masks, centered in the image and featuring a 20-pixel margin around each edge, were used for this process. For SG2IM, which utilizes scene graphs as input, we converted these from SPRING's propositional logic without ambiguity. It is worth noting that during our evaluation, we found that the images generated by SG2IM were of low quality and displayed minimal variations when given the same scene graph. We maintained consistency with the parameters and code provided in the original SG2IM paper. After reaching out to the author via GitHub, we learned that the poor image quality was likely due to mode collapse. Nevertheless, we included these results in our evaluation for a comprehensive comparison. Background images were generated by the algorithms themselves, increasing the difficulty of the task. SPRING handles this by using the VEG with the prompt "a clean, empty, living room." or "a clean, empty, kitchen.". Stable Diffusion used the same approach, generating a background before receiving the specification and then inpainting it to complete the task. As SG2IM inherently generates its own backgrounds, this aspect remains consistent with its

Figure 6: Images produced by SPRING with generated backgrounds and no positional constraints – only objects are specified. SPRING's SRM still finds sensible locations for objects, even in the absence of complex constraints. The list of objects generated for each image here can be found in Appendix A.3.

usual operation. The primary metrics we collect here are the Inception score (IS) [56] and Fréchet Inception Distance (FID) [30]. These are measures of the quality and diversity of images from a generative model based on the intermediate layers of a pre-trained classifier. For IS, higher scores indicate better quality images, while FID scores indicate better quality with lower scores. FID also requires comparison statistics to a control dataset – in our case, COCO 2017. Both metrics are known to be volatile and sometimes inaccurate [6]. Once compiled, all images are resized to 1000x1000 to make a fair comparison (IS and FID scores are effected by image size). Scene Inception Scores are generated using our bounding boxes to isolate each object and score them independently. More detailed information on experimental setup can be found in Appendix A.

Results. Interior designs from various background images (collected from across the web, generated and COCO examples can be found in Appendix B) can be viewed in Figures 4, 5, and 6. These images are qualitatively as good or superior to baselines, and they are able to satisfy the given constraints. Quantitative results are presented in Table 3. SPRING received superior scores in both metrics.

5.2 Evaluating Design Adherence

Setup. To evaluate the performance of each method, 20 interior designs were generated using randomly-generated specifications (see Appendix A.1) and backgrounds from COCO's test set. Each specification included 3 objects and 4 constraints. The designs were visually inspected by the author, and object accuracy and position accuracy were measured as follows: *Object accuracy.* the author counted and classified the objects in each image. If all 3 objects were visible and identifiable, the image was given a 100% object accuracy. Two identifiable objects resulted in a 67% accuracy, and so on. This score was then averaged across all 20 images to measure the object accuracy of the method. *Position accuracy.* for each constraint clause (e.g. the oven is left of the toaster), the author checked whether the constraint was clearly true within the image. Clauses that referenced images which were not inpainted correctly (penalized in object accuracy) were not included in this count, only relationships between visible and recognizable objects. Position accuracy was also averaged across all 20 images to produce our final metrics. SPRING does not guarantee perfect object accuracy, but improves it by explicitly painting one object at a time in isolation from others. SPRING does guarantee perfect position accuracy via the forward checking procedure in the SRM.

property(3,"A big red flower") ∧ property(4,"A green leafy fern") ∧
(atop(3,1) ∧ atop(4,0)) ∨ (atop(3,2) ∧ atop(4,1))

Figure 7: SPRING's zero-shot transfer learning performance on a new constraint `atop` never present in the training set. `atop` constrains an object to be sitting on top of another. This specification applies to all backgrounds which already have three tables: 0, 1, and 2 from left to right. The flower is always one table to the right of the green fern, showing good performance of SPRING. More detail on `atop` and adding constraints zero-shot can be found in Appendix C.

Results. All metrics are presented in Table 3. Stable Diffusion had lower object accuracy than SPRING, and also showed much worse position accuracy compared to SPRING (50% for Stable Diffusion alone compared to 100% with SPRING). Identifying objects was not possible with SG2IM hence its accuracy is 0.

5.3 Evaluating Spatial Reasoning

Setup. This experiment assesses how well generated object locations satisfy explicit user specifications and implicit preferences, which are hard to measure in real-world datasets. We define three synthetic scenarios with known object location distributions, known to the programmer but not the algorithm. No VEG or perception module is used. We evaluate *preference accuracy* as the percentage of generated locations meeting implicit preferences. See Appendix E.2 for scenario specifications. We compare SPRING planning with a GAN augmented with a convex optimization layer (details are discussed in Appendix E.1), which also combines reasoning and deep learning but has a less rich constraint set. Both methods are trained on each scenario until convergence, and each dataset is matched with a set of constraints during testing.

Results. As shown in Table 2, the SRM formulation SPRING uses outperformed or matched GAN + CVX in preference accuracy for every dataset. Both algorithms guarantee positional constraints, but GAN + CVX only does this with convex constraints.

5.4 Human Study

Setup. In this study, we compared our SPRING method and Stable Diffusion inpainting for generating interior space images, like kitchens, living rooms, and billiard rooms. Participants were provided with a background image, a completed scene, and a bullet-pointed specification used to generate the image. Additionally, questions with images generated by SPRING displayed the intermediate layout. Background images were generated using the methods described previously. Constraints were handcrafted by the authors to fit the background.

Participants were asked to rate each image on a 5-point Likert scale across four distinct metrics: specification satisfaction, aesthetic appeal, background preservation, spatial naturalness. For specification satisfaction, they assessed how well the image adhered to the specifications, including object visibility, constraint satisfaction, and details such as color, texture, and material. Aesthetic appeal evaluated the overall quality of the image, regardless of its adherence to the prompt. Background preservation required participants to consider how well the original background was maintained without unnecessary alterations or damage. Lastly, spatial naturalness considered the proportions between objects, the proportions between an object and the background, and the natural placement of objects for their respective types. More details on the study can be found in Appendix F.

Results. The averaged results are presented in Table 4. Our findings indicate that SPRING nearly matches the aesthetic quality and spatial naturalness of Stable Diffusion, as anticipated. Furthermore, SPRING significantly outperforms Stable Diffusion in terms of specification satisfaction and background preservation. These results demonstrate the effectiveness of the SPRING method for generating high-quality interior space images that adhere closely to the provided specifications while maintaining the integrity of the original background.

6 Conclusion

In this work, we introduced SPRING for design production. Good designs must meet specific user requirements and comply with implicit guidelines on appearance and functionality. We achieve this by integrating neural generative models with constraint reasoning. The object positions suggested by the neural network are filtered through constraint reasoning-based forward checking to meet user specifications. Our SPRING produces high-quality interior design scenes that respect user-defined spatial requirements, satisfy common sense and look pleasing. Our approach also handles new constraint types in a zero-shot manner due to the forward checker's programmability. It is also more interpretable as decisions are made iteratively. The main limitation of our work is the dependence on the VEG model's quality and compatibility for object generation. Future work will focus on enhancing control between the SRM and VEG and adapting to other domains, such as 3D design.

References

[1] Akshay Agrawal, Brandon Amos, Shane Barratt, Stephen Boyd, Steven Diamond, and J. Zico Kolter. Differentiable convex optimization layers. In *Advances in Neural Information Processing Systems*, pages 9558–9570, 2019.

[2] Akshay Agrawal, Shane Barratt, and Stephen Boyd. Learning convex optimization models. *IEEE/CAA Journal of Automatica Sinica*, 8(8):1355–1364, 2021.

[3] Akshay Agrawal, Shane Barratt, Stephen Boyd, and Bartolomeo Stellato. Learning convex optimization control policies. In Alexandre M. Bayen, Ali Jadbabaie, George Pappas, Pablo A. Parrilo, Benjamin Recht, Claire Tomlin, and Melanie Zeilinger, editors, *Proceedings of the 2nd Conference on Learning for Dynamics and Control*, volume 120 of *Proceedings of Machine Learning Research*, pages 361–373. PMLR, 10–11 Jun 2020.

[4] Thomas Anthony, Zheng Tian, and David Barber. Thinking fast and slow with deep learning and tree search. In I. Guyon, U. Von Luxburg, S. Bengio, H. Wallach, R. Fergus, S. Vishwanathan, and R. Garnett, editors, *Advances in Neural Information Processing Systems*, volume 30. Curran Associates, Inc., 2017.

[5] Yiwei Bai, Di Chen, and Carla P. Gomes. CLR-DRNets: Curriculum Learning with Restarts to Solve Visual Combinatorial Games. In Laurent D. Michel, editor, *27th International Conference on Principles and Practice of Constraint Programming (CP 2021)*, volume 210 of *Leibniz International Proceedings in Informatics (LIPIcs)*, pages 17:1–17:14, Dagstuhl, Germany, 2021. Schloss Dagstuhl – Leibniz-Zentrum für Informatik.

[6] Shane Barratt and Rishi Sharma. A note on the inception score. *arXiv preprint arXiv:1801.01973*, 2018.

[7] Andrea Bartolini, Michele Lombardi, Michela Milano, and Luca Benini. Neuron constraints to model complex real-world problems. In *Principles and Practice of Constraint Programming–CP 2011: 17th International Conference, CP 2011, Perugia, Italy, September 12-16, 2011. Proceedings 17*, pages 115–129. Springer, 2011.

[8] Christian Bessiere, Frédéric Koriche, Nadjib Lazaar, and Barry O'Sullivan. Constraint acquisition. *Artificial Intelligence*, 244:315–342, 2017. Combining Constraint Solving with Mining and Learning.

[9] Christian Bessière, Luc de Raedt, Tias Guns, Lars Kotthoff, Mirco Nanni, Siegfried Nijssen, Barry O'Sullivan, Anastasia Paparrizou, Dino Pedreschi, and Helmut Simonis. The Inductive Constraint Programming Loop. *IEEE Intelligent Systems*, 2018.

[10] Grady Booch, Francesco Fabiano, Lior Horesh, Kiran Kate, Jonathan Lenchner, Nick Linck, Andreas Loreggia, Keerthiram Murgesan, Nicholas Mattei, Francesca Rossi, et al. Thinking fast and slow in ai. In *Proceedings of the AAAI Conference on Artificial Intelligence*, volume 35, pages 15042–15046, 2021.

[11] Andrea Borghesi, Federico Baldo, and Michela Milano. Improving deep learning models via constraint-based domain knowledge: a brief survey. *arXiv preprint arXiv:2005.10691*, 2020.

[12] Stephen Boyd and Lieven Vandenberghe. *Convex optimization*. Cambridge university press, 2004.

[13] Nicolas Carion, Francisco Massa, Gabriel Synnaeve, Nicolas Usunier, Alexander Kirillov, and Sergey Zagoruyko. End-to-end object detection with transformers. *CoRR*, abs/2005.12872, 2020.

[14] Kai-Hung Chang, Chin-Yi Cheng, Jieliang Luo, Shingo Murata, Mehdi Nourbakhsh, and Yoshito Tsuji. Building-gan: Graph-conditioned architectural volumetric design generation. In *Proceedings of the IEEE/CVF International Conference on Computer Vision (ICCV)*, pages 11956–11965, October 2021.

[15] Di Chen, Yiwei Bai, Sebastian Ament, Wenting Zhao, Dan Guevarra, Lan Zhou, Bart Selman, R Bruce van Dover, John M Gregoire, and Carla P Gomes. Automating crystal-structure phase mapping by combining deep learning with constraint reasoning. *Nature Machine Intelligence*, 3(9):812–822, 2021.

[16] Zixuan Chen and Xiang Wang. Application of ai technology in interior design. In *E3S Web of Conferences*, volume 179, page 02105. E3S Web of Conferences, 2020.

[17] Kyunghyun Cho, Bart van Merrienboer, Dzmitry Bahdanau, and Yoshua Bengio. On the properties of neural machine translation: Encoder–decoder approaches. In *SSST@EMNLP*, 2014.

[18] Fei Deng, Zhuo Zhi, Donghun Lee, and Sungjin Ahn. Generative scene graph networks. In *International Conference on Learning Representations*, 2021.

[19] Jia Deng, Wei Dong, Richard Socher, Li-Jia Li, Kai Li, and Li Fei-Fei. Imagenet: A large-scale hierarchical image database. In *2009 IEEE conference on computer vision and pattern recognition*, pages 248–255. Ieee, 2009.

[20] Fabrizio Detassis, Michele Lombardi, and Michela Milano. Teaching the old dog new tricks: Supervised learning with constraints. In *Proceedings of the AAAI Conference on Artificial Intelligence*, volume 35, pages 3742–3749, 2021.

[21] Helisa Dhamo, Azade Farshad, Iro Laina, Nassir Navab, Gregory D Hager, Federico Tombari, and Christian Rupprecht. Semantic image manipulation using scene graphs. In *Proceedings of the IEEE/CVF conference on computer vision and pattern recognition*, pages 5213–5222, 2020.

[22] Sašo Džeroski, Luc De Raedt, and Hendrik Blockeel. Relational reinforcement learning. In *Inductive Logic Programming: 8th International Conference, ILP-98 Madison, Wisconsin, USA, July 22–24, 1998 Proceedings 8*, pages 11–22. Springer, 1998.

[23] Martin Engelcke, Adam R. Kosiorek, Oiwi Parker Jones, and Ingmar Posner. Genesis: Generative scene inference and sampling with object-centric latent representations. In *International Conference on Learning Representations*, 2020.

[24] Jonathan St BT Evans. In two minds: dual-process accounts of reasoning. *Trends in cognitive sciences*, 7(10):454–459, 2003.

[25] Francesco Fabiano, Vishal Pallagani, Marianna Bergamaschi Ganapini, Lior Horesh, Andrea Loreggia, Keerthiram Murugesan, Francesca Rossi, and Biplav Srivastava. Fast and slow planning, 2023.

[26] M. Bergamaschi Ganapini, Murray Campbell, Francesco Fabiano, Lior Horesh, Jon Lenchner, Andrea Loreggia, Nicholas Mattei, Francesca Rossi, Biplav Srivastava, and Kristen Brent Venable. Thinking fast and slow in ai: The role of metacognition. In Giuseppe Nicosia, Varun Ojha, Emanuele La Malfa, Gabriele La Malfa, Panos Pardalos, Giuseppe Di Fatta, Giovanni Giuffrida, and Renato Umeton, editors, *Machine Learning, Optimization, and Data Science*, pages 502–509, Cham, 2023. Springer Nature Switzerland.

[27] Sarthak Garg, Helisa Dhamo, Azade Farshad, Sabrina Musatian, Nassir Navab, and Federico Tombari. Unconditional scene graph generation. In *Proceedings of the IEEE/CVF International Conference on Computer Vision*, pages 16362–16371, 2021.

[28] Kaiming He, Xiangyu Zhang, Shaoqing Ren, and Jian Sun. Deep Residual Learning for Image Recognition. In *Proceedings of 2016 IEEE Conference on Computer Vision and Pattern Recognition*, CVPR '16, pages 770–778. IEEE, June 2016.

[29] Pengcheng He, Xiaodong Liu, Weizhu Chen, and Jianfeng Gao. A hybrid neural network model for commonsense reasoning. In *Proceedings of the First Workshop on Commonsense Inference in Natural Language Processing*, pages 13–21, Hong Kong, China, November 2019. Association for Computational Linguistics.

[30] Martin Heusel, Hubert Ramsauer, Thomas Unterthiner, Bernhard Nessler, and Sepp Hochreiter. Gans trained by a two time-scale update rule converge to a local nash equilibrium. In I. Guyon, U. Von Luxburg, S. Bengio, H. Wallach, R. Fergus, S. Vishwanathan, and R. Garnett, editors, *Advances in Neural Information Processing Systems*, volume 30. Curran Associates, Inc., 2017.

[31] Kwang Hyuk Im and Sang Chan Park. Case-based reasoning and neural network based expert system for personalization. *Expert Systems with Applications*, 32(1):77–85, 2007.

[32] Nan Jiang, Maosen Zhang, Willem-Jan van Hoeve, and Yexiang Xue. Constraint reasoning embedded structured prediction. *Journal of Machine Learning Research*, 23(345):1–40, 2022.

[33] Justin Johnson, Agrim Gupta, and Li Fei-Fei. Image generation from scene graphs. In *CVPR*, 2018.

[34] Daniel Kahneman. *Thinking, fast and slow*. Farrar, Straus and Giroux, New York, 2011.

[35] Brucek Khailany, Haoxing Ren, Steve Dai, Saad Godil, Ben Keller, Robert Kirby, Alicia Klinefelter, Rangharajan Venkatesan, Yanqing Zhang, Bryan Catanzaro, et al. Accelerating chip design with machine learning. *IEEE Micro*, 40(6):23–32, 2020.

[36] Elias Khalil, Hanjun Dai, Yuyu Zhang, Bistra Dilkina, and Le Song. Learning combinatorial optimization algorithms over graphs. *Advances in neural information processing systems*, 30, 2017.

[37] Gaurav Kumar, Ashish Kumar, and Rahul. A deep learning approach for interior designing of apartment building architecture using u2 net. In *2022 International Conference on Sustainable Computing and Data Communication Systems (ICSCDS)*, pages 1465–1471, 2022.

[38] Luís C. Lamb, Artur d'Avila Garcez, Marco Gori, Marcelo O.R. Prates, Pedro H.C. Avelar, and Moshe Y. Vardi. Graph neural networks meet neural-symbolic computing: A survey and perspective. In Christian Bessiere, editor, *Proceedings of the Twenty-Ninth International Joint Conference on Artificial Intelligence, IJCAI-20*, pages 4877–4884. International Joint Conferences on Artificial Intelligence Organization, 7 2020. Survey track.

[39] Yann LeCun. A path towards autonomous machine intelligence version 0.9. 2, 2022-06-27. *Open Review*, 62, 2022.

[40] Xinrong Li, Hong Li, Chiyu Wang, Xun Hu, and Wei Zhang. Visual-attention gan for interior sketch colourisation. *IET Image Processing*, 15(4):997–1007, 2021.

[41] Tsung-Yi Lin, Michael Maire, Serge Belongie, James Hays, Pietro Perona, Deva Ramanan, Piotr Dollár, and C Lawrence Zitnick. Microsoft coco: Common objects in context. In *European conference on computer vision*, pages 740–755. Springer, 2014.

[42] Wei-Lun Lin and Yunn-Wen Lien. The different role of working memory in open-ended versus closed-ended creative problem solving: A dual-process theory account. *Creativity Research Journal*, 25(1):85–96, 2013.

[43] Nan Liu, Shuang Li, Yilun Du, Josh Tenenbaum, and Antonio Torralba. Learning to compose visual relations. *Advances in Neural Information Processing Systems*, 34:23166–23178, 2021.

[44] Michele Lombardi and Michela Milano. Boosting combinatorial problem modeling with machine learning. *arXiv preprint arXiv:1807.05517*, 2018.

[45] Maxime Mulamba, Emilio Gamba, and Tias Guns. Decision focused learning for prediction + optimisation problems. In *Proceedings of AAAI, Constraint Programming and Machine Learning Bridge Program*, 2023.

[46] Nelson Nauata, Kai-Hung Chang, Chin-Yi Cheng, Greg Mori, and Yasutaka Furukawa. House-gan: Relational generative adversarial networks for graph-constrained house layout generation. In *European Conference on Computer Vision*, pages 162–177. Springer, 2020.

[47] Nelson Nauata, Sepidehsadat Hosseini, Kai-Hung Chang, Hang Chu, Chin-Yi Cheng, and Yasutaka Furukawa. House-gan++: Generative adversarial layout refinement network towards intelligent computational agent for professional architects. In *Proceedings of the IEEE/CVF Conference on Computer Vision and Pattern Recognition*, pages 13632–13641, 2021.

[48] Alex Nichol, Prafulla Dhariwal, Aditya Ramesh, Pranav Shyam, Pamela Mishkin, Bob McGrew, Ilya Sutskever, and Mark Chen. Glide: Towards photorealistic image generation and editing with text-guided diffusion models, 2021.

[49] Baolin Peng, Zhengdong Lu, Hang Li, and Kam-Fai Wong. Towards neural network-based reasoning. *ArXiv*, abs/1508.05508, 2015.

[50] Anil Audumbar Pise, Hima Vadapalli, and Ian Sanders. Relational reasoning using neural networks: A survey. *International Journal of Uncertainty, Fuzziness and Knowledge-Based Systems*, 29(Supp02):237–258, 2021.

[51] Steven D Prestwich, Eugene C Freuder, Barry O'Sullivan, and David Browne. Classifier-based constraint acquisition. *Annals of Mathematics and Artificial Intelligence*, 89:655–674, 2021.

[52] Aditya Ramesh, Prafulla Dhariwal, Alex Nichol, Casey Chu, and Mark Chen. Hierarchical text-conditional image generation with clip latents. *arXiv preprint arXiv:2204.06125*, 2022.

[53] Aditya Ramesh, Mikhail Pavlov, Gabriel Goh, Scott Gray, Chelsea Voss, Alec Radford, Mark Chen, and Ilya Sutskever. Zero-shot text-to-image generation. In Marina Meila and Tong Zhang, editors, *Proceedings of the 38th International Conference on Machine Learning*, volume 139 of *Proceedings of Machine Learning Research*, pages 8821–8831. PMLR, 18–24 Jul 2021.

[54] Robin Rombach, Andreas Blattmann, Dominik Lorenz, Patrick Esser, and Björn Ommer. High-resolution image synthesis with latent diffusion models, 2021.

[55] Louis-Martin Rousseau, Michel Gendreau, and Gilles Pesant. Using constraint-based operators to solve the vehicle routing problem with time windows. *Journal of heuristics*, 8:43–58, 2002.

[56] Tim Salimans, Ian Goodfellow, Wojciech Zaremba, Vicki Cheung, Alec Radford, and Xi Chen. Improved techniques for training gans. *Advances in neural information processing systems*, 29, 2016.

[57] Adam Santoro, David Raposo, David G Barrett, Mateusz Malinowski, Razvan Pascanu, Peter Battaglia, and Timothy Lillicrap. A simple neural network module for relational reasoning. In I. Guyon, U. Von Luxburg, S. Bengio, H. Wallach, R. Fergus, S. Vishwanathan, and R. Garnett, editors, *Advances in Neural Information Processing Systems*, volume 30. Curran Associates, Inc., 2017.

[58] Jascha Sohl-Dickstein, Eric Weiss, Niru Maheswaranathan, and Surya Ganguli. Deep unsupervised learning using nonequilibrium thermodynamics. In Francis Bach and David Blei, editors, *Proceedings of the 32nd International Conference on Machine Learning*, volume 37 of *Proceedings of Machine Learning Research*, pages 2256–2265, Lille, France, 07–09 Jul 2015. PMLR.

[59] Paul T. Sowden, Andrew Pringle, and Liane Gabora. The shifting sands of creative thinking: Connections to dual-process theory. *Thinking & Reasoning*, 21(1):40–60, 2015.

[60] Tristan Sylvain, Pengchuan Zhang, Yoshua Bengio, R Devon Hjelm, and Shikhar Sharma. Object-centric image generation from layouts. In *Proceedings of the AAAI Conference on Artificial Intelligence*, volume 35, pages 2647–2655, 2021.

[61] Alexandru Telea. An image inpainting technique based on the fast marching method. *Journal of graphics tools*, 9(1):23–34, 2004.

[62] Trieu H. Trinh and Quoc V. Le. A simple method for commonsense reasoning, 2018.

[63] Dimosthenis C. Tsouros, Tias Guns, and Kostas Stergiou. Learning constraint models from data. In *Proceedings of AAAI, Constraint Programming and Machine Learning Bridge Program*, 2023.

[64] Ashish Vaswani, Noam Shazeer, Niki Parmar, Jakob Uszkoreit, Llion Jones, Aidan N Gomez, Łukasz Kaiser, and Illia Polosukhin. Attention is all you need. *Advances in neural information processing systems*, 30, 2017.

[65] Michael Jeffrey Volk, Ismini Lourentzou, Shekhar Mishra, Lam Tung Vo, Chengxiang Zhai, and Huimin Zhao. Biosystems design by machine learning. *ACS synthetic biology*, 9(7):1514–1533, 2020.

[66] Kai Wang, Sanket Shah, Haipeng Chen, Andrew Perrault, Finale Doshi-Velez, and Milind Tambe. Learning mdps from features: Predict-then-optimize for sequential decision making by reinforcement learning. In M. Ranzato, A. Beygelzimer, Y. Dauphin, P.S. Liang, and J. Wortman Vaughan, editors, *Advances in Neural Information Processing Systems*, volume 34, pages 8795–8806. Curran Associates, Inc., 2021.

[67] Ningqi Wang, Chang Niu, and Zizhong Li. Rlayout: Interior design system based on reinforcement learning. In *2019 12th International Symposium on Computational Intelligence and Design (ISCID)*, volume 1, pages 117–120, 2019.

[68] Ronald J. Williams and David Zipser. A learning algorithm for continually running fully recurrent neural networks. *Neural Computation*, 1(2):270–280, 1989.

[69] Kun Xu, Haoyu Liang, Jun Zhu, Hang Su, and Bo Zhang. Deep structured generative models. *arXiv preprint arXiv:1807.03877*, 2018.

[70] Yexiang Xue and Willem-Jan van Hoeve. Embedding decision diagrams into generative adversarial networks. In *International Conference on Integration of Constraint Programming, Artificial Intelligence, and Operations Research*, pages 616–632. Springer, 2019.

[71] Yuji Yoshimura, Bill Cai, Zhoutong Wang, and Carlo Ratti. *Deep Learning Architect: Classification for Architectural Design Through the Eye of Artificial Intelligence*, pages 249–265. Springer International Publishing, Cham, 2019.

[72] Vinicius Zambaldi, David Raposo, Adam Santoro, Victor Bapst, Yujia Li, Igor Babuschkin, Karl Tuyls, David Reichert, Timothy Lillicrap, Edward Lockhart, et al. Relational deep reinforcement learning. *arXiv preprint arXiv:1806.01830*, 2018.

[73] Alireza Zareian, Zhecan Wang, Haoxuan You, and Shih-Fu Chang. Learning visual commonsense for robust scene graph generation. In *European Conference on Computer Vision*, pages 642–657. Springer, 2020.

[74] Bo Zhao, Lili Meng, Weidong Yin, and Leonid Sigal. Image generation from layout. In *Proceedings of the IEEE/CVF Conference on Computer Vision and Pattern Recognition*, pages 8584–8593, 2019.

A General Additional Experiment Details

A.1 How Random Specifications Were Generated

In order to conduct fair evaluations in sections 5.1 and 5.2, user specifications were generated randomly using the following procedure. For ease of generation, only the constraints cleft, cright, cabove, and cbelow could be sampled. Possible object types were selected based on the room being generated – chair, couch, potted plant, dining table, and television for living rooms; microwave, oven, toaster, refrigerator, and potted plant for kitchens. A requested number of objects and constraints were selected for each scene, with replacement, and each specification generated was checked to ensure it was satisfiable. Additionally, natural language prompts were generated programmatically for use with the Stable Diffusion and GLIDE baselines. These prompts listed all objects and defined each constraint, for example, "An oven, a refrigerator, and a toaster. The toaster is left of the oven. The refrigerator is above the oven…". These specifications were also logged as scene graphs for use by SG2IM. The conversion from our language to scene graphs was done without ambiguity or information loss.

A.2 Using the COCO Dataset

As previously stated in the main text, the COCO 2017 Detection dataset was utilized to train SPRING. It is also utilized in the extended evaluation below. To ensure that the dataset was focused on interior design, only images including one or more of the following categories were included: chair, couch, potted plant, bed, mirror, dining table, window, desk, toilet, door, tv, microwave, oven, toaster, sink, refrigerator, or blender. In order to train SPRING in a supervised manner, it was necessary to remove these objects from the images, leaving only the empty backgrounds and bounding box annotations. To accomplish this, various methods were tested with the goal of achieving visually pleasing results while also being efficient as numerous images needed to be processed. The Telea method was ultimately selected as it uses an image's gradient information to guide the inpainting process, resulting in visually plausible results. The algorithm works by first defining the region to be removed, and then using an iterative algorithm to fill in the region with a combination of the pixels surrounding the hole and the image's gradient information. The filtered and Telea-processed version of the dataset will be made available at the time of publication to aid in reproducibility.

A.3 Logical Language Translation

The logical instructions to generate the figures in this work is given in Table 5. Note the relation `default`, which combines a number of default constraints used on all objects to fit the limitations of the VEG module. For the Stable Diffusion figures, the objects are set to have a width and height between 256 and 512 pixels. Additionally, the bounding boxes for these objects are constrained such that they do not extend beyond the boundaries of the image. For the GLIDE figures, the same default constraints are used, with the exception that the objects are bounded between 150 and 256 pixels. This does not include Figure 6, which has its objects described for each image in Table 6 – as that figure does not include positional constraints beyond the default.

Logic Language	**Natural Language**
type(0,"oven") ∧ property(0,"a modern looking oven") ∧ default(0) ∧ right_value(0, 400)	Add a modern looking oven in the middle or right side.
# 0: a microwave, 1: an oven. type(2,"toaster") ∧ type(3,"plant") ∧ property(2,"a retro toaster oven") ∧ property(3,"a potted potato plant") ∧ default(2) ∧ default(3) ∧ xeq(2,0) ∧ yeq(2,0) ∧ wider(2,0) ∧ taller(2,0) ∧ cbelow(3,0) above(3,1)	Replace the microwave with a retro toaster oven and add a potted potato plant fully below the toaster oven and at least partly above the oven.
# 0: a chair. type(1,"chair") ∧ type(2,"table") ∧ property(1,"a dark colored leather chair") ∧ property(2,"a wooden table") ∧ default(1) ∧ default(2) ∧ cleft(1,0,300) ∧ below(2,1) ∧ below(2,0) ∧ left(2,0) ∧ right(2,1,100)	Add a dark colored leather chair fully left of the white chair, and a wooden table between and below them.
type(0,"tv") ∧ type(1,"couch") ∧ type(2,"chair") ∧ property(0,"a flat screen tv") ∧ property(1,"a couch facing left") ∧ property(2,"a chair") ∧ default(0) ∧ default(1) ∧ default(2) ∧ left_value(0,150) ∧ cright(1,0) ∧ cright(2,0) ∧ cabove(2,1)	Add a flat screen TV in the left 15% of the image. Also add a red chair and a couch right of the TV, where the chair is above the couch.
# 0: a tv. type(1,"chair") ∧ type(2,"couch") ∧ type(3,"chair") ∧ property(1,"a red chair facing away") ∧ property(2,"a couch facing away") ∧ property(3,"a blue chair facing away") ∧ default(1) ∧ default(2) ∧ default(3) ∧ cbelow(1,0) ∧ yeq(2,1) ∧ yeq(3,1) ∧ cleft(1,2) ∧ cleft(2,3)	Add a blue chair, a couch, and a red chair, left to right, all under the TV.
type(0,"microwave") ∧ type(1,"oven") ∧ property(0,"a blue microwave") ∧ property(1,"a black oven") ∧ default(0) ∧ default(1) ∧ cabove(0, 1)	A blue microwave above a black oven.
type(0,"microwave") ∧ type(1,"oven") ∧ type(2,"refrigerator") ∧ default(0) ∧ default(1) ∧ default(2) ∧ cleft(2,1) ∧ cright(0,1) ∧ cabove(0,1)	A refrigerator left of an oven and a microwave right and above the same oven.
# 0: a sink, 1: an oven. type(2,"microwave") ∧ type(3,"toaster") ∧ property(2,"a blue microwave") ∧ property(3,"a green toaster") ∧ default(2) ∧ default(3) ∧ cright(2,1) ∧ cleft(3,1) ∧ cbelow(3,0)	Add a blue microwave right of the oven, and a green toaster left of the oven and below the sink.

Table 5: The logic formulations used for figures in this work with accompanying descriptive text. '#' comments represent objects that were detected by the perception module and incorporated.

microwave, potted plant
microwave, plant
microwave, oven
toaster, plant
toaster, plant
couch, table
chair, table
plant, chair
couch, table
couch, tv
chair, plant, table
chair, table
couch, chair, plant
couch, chair, table,
chair, table
microwave, refrigerator
microwave, refrigerator, oven
refrigerator, microwave
oven, toaster, toaster
microwave, refrigerator, toaster
toaster, oven, refrigerator
plant, tv, table
plant, couch
chair, table
couch, tv, plant
refrigerator, refrigerator, oven
sink, toaster, microwave
sink, toaster, oven
microwave, microwave, oven
microwave, toaster
microwave, refrigerator, refrigerator
plant, couch, table
couch, chair, table
chair, table
chair, chair, table
oven, refrigerator, microwave
microwave, oven, refrigerator
oven, plant,
couch, couch, table
couch, chair

Table 6: Objects generated for Figure 6, listed from top left to bottom right. These images do not contain positional constraints, and show that the SPRING's spatial reasoning module can provide good locations for objects even without human planning and closely tailored specifications.

Figure 8: A closer look at some of the images generated for Figures 1 and 2. Note that the background is minimally disturbed. Also note that, while the microwave can be anywhere right of the oven, it is placed in a reasonable place – on the counter or built into the cabinets.

B Extended Image Quality Experimental Details

This section provides an extended analysis of our experimental results, including evaluation on additional real images from the COCO dataset and generated images. Moreover, we also test GLIDE as a baseline and as a backbone for SPRING's VEG module, both for its performance and in comparison to Stable Diffusion.

B.1 Additional Evaluation Sets

In addition to our primary experiment, we conducted evaluations on smaller sets that included both real images from the COCO dataset and generated images. We tested GLIDE, which shares a similar structure to Stable Diffusion, alongside the latter. GLIDE was not included in the main experimental section due to computational resource constraints (our SRM and perception modules run very quickly, usually under 1 second, but diffusion models take a long time to run even during inference) and space limitations. As Stable Diffusion has been fully released, we opted to use it in our main experiments, whereas GLIDE is only available through its "reduced and filtered" version.

For the extended evaluations, we generated 100 images per method and tested 100 random kitchen images from the COCO dataset. This is not ideal for the metrics calculated, but the primary experiment addresses that with far more images at the cost of significant resource usage. We also tested GLIDE both as a standalone baseline and as a backbone for SPRING's VEG module.

B.2 Impact of VEG Choice on Accuracy

Our results show that SPRING achieved perfect position accuracy regardless of the VEG choice. This makes sense as position accuracy is determined almost solely by the Spatial Reasoning Module, which guarantees constraint satisfaction through the forward checker. However, the VEG choice did affect object accuracy due to the possibility of inpaint failures. The Stable Diffusion-based VEG had significantly fewer inpaint failures than the GLIDE-based VEG.

B.3 Scene Inception Score

We calculated the Scene Inception score (ScIS) [60] for SPRING, a metric that measures the quality of individual objects in the generated scenes. This metric was not easily calculated for other methods, as it requires measuring objects in isolation. SPRING's convenient layouts made it feasible to calculate ScIS, while it was more challenging for the other tested methods.

Method	Position Accuracy ↑	Object Accuracy ↑	Real BG		Gen BG	
			IS ↑	ScIS ↑	IS ↑	ScIS ↑
Stable Diffusion	0.5	0.63	2.45	n/a	2.54	n/a
GLIDE	0.24	0.35	2.83	n/a	2.56	n/a
sg2im	0.0	0.0	n/a	n/a	**3.28**	n/a
SPRING[SD] ⋆	**1.0**	**0.77**	**3.50**	4.75	2.40	4.56
SPRING[G] ⋆	**1.0**	0.46	3.33	**5.31**	2.08	**4.80**

Table 7: Quantitative results on the COCO dataset. Inception Score (IS) and Scene Inception Score (ScIS) indicate image quality. Position accuracy represents how often the positional constraints are met. Object accuracy represents how often the correct number and type of objects are generated and identifiable. Our SPRING has comparable scores in image quality with the state of the art (IS and ScIS), while satisfying constraints (high position and object accuracies).

B.4 Extended Results

Table 7 provides an overview of the extended results, including position accuracy, object accuracy, and inception scores (IS) for both real and generated backgrounds. ScIS scores are also included where applicable. SPRING with Stable Diffusion (SPRING[SD]) achieved the best overall results, with perfect position accuracy and the highest object accuracy. The Inception scores for real backgrounds were also superior compared to other methods, while the generated background results were competitive with other approaches. SG2IM receives a much higher result than expected for generated background inception scoring. However, this is likely only due to the small testing set, as this advantage drops away in the primary experiment, which uses 10,000 generated examples. SPRING with GLIDE (SPRING[G]) also demonstrated perfect position accuracy, but had lower object accuracy due to more frequent inpaint failures.

C Demonstrating Zero-shot Constraint Satisfaction

Our approach allows for re-programming of the forward checker for zero-shot constraint editing. New constraints can be implemented and used in filtering the GRU outputs of the SRM at any time, even after training. To demonstrate this capability, we construct a new constraint type after training SPRING. We define this constraint as $\texttt{atop}(o_1, o_2)$ – which constrains the first object's bounding box (o_1) to be on top of the first object's bounding box (o_2). More precisely, `atop` evaluates to true if and only if:

- the bottom of the first object's bounding box is between the top and the bottom of the second object's bounding box.
- the right side of the first object's bounding box is between the right and left sides of the second object's bounding box.
- the top of the first object's bounding box is above the top of the second object's bounding box.

By combining this new constraint with the previous language set, very complex specifications can be produced. In Figure 7 in the main text, `atop` is used to define a complex specification utilizing the perception module to create a design which can be applied to any background including three tables. A flower and a fern are to be placed in the image. The flower is always one table to the right of the green fern (e.g. if the fern is on the middle table, the flower is on the right table, and if the fern is on the left table, the flower is on the middle table). As demonstrated in that figure, specifications can be automatically applied to entire sets of backgrounds, and produce diverse and complex images through use of zero-shot constrains.

D Architectures, Training, and Hyperparameters

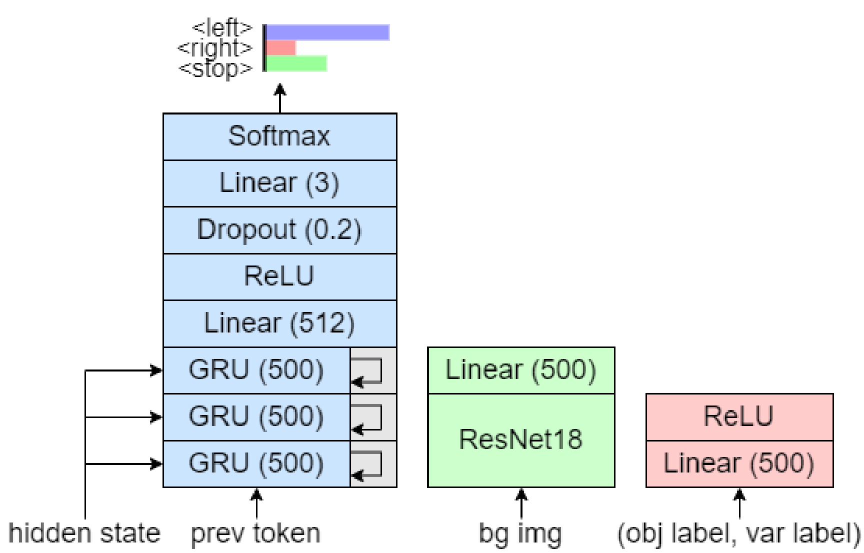

Figure 9: The recurrent network (left), scene encoder (center), and variable encoder (right) of the spatial reasoning net. These networks together allow our method to make sequential decisions on the position of objects in the design.

D.1 Architectures

SPRING is composed of a perception module, a spatial reasoning module, and a visual element generator. The object detector network within the perception module as well as the VEG both make use of pre-trained and pre-defined modules from other papers, so this section will focus on the spatial reasoning module. The primary network of the SRM is made up of 3 gated recurrent units followed by a dense layer, and a Softmax activated output layer. GRUs use a hidden state to preserve information across time, and manage that information using internal reset and update gates. This hidden state is initialized from a vector produced by the scene encoder. The scene encoder is a pretrained ResNet18 backbone augmented with a dense layer. The purpose of this network is to extract features from the scene as a whole. The hidden state is also updated by a simple variable encoder, which produces a vector for each positional variable of each object to let the GRUs know that a new object or variable has started, and to encode the object class and variable type.

D.2 Training

In training the SRM, much work went into deciding a training strategy. It is accomplished through *teacher forcing* [68]. In teacher forcing, the ground truth decision token from the previous step drawn from the training set is used as the input to train the RNN to predict the decision of the current step. Teacher forcing can drastically speed up RNN training, but can also result in lower resilience to uncommon sequences. For this reason, a mixture of strategies – with and without teacher forcing – is used to train the model. 50% of the time the input of the RNN is set by teacher forcing and 50% set by the predictions of the RNN itself. We also randomize the order of the objects in the decision string during training. SPRING was trained with a learning rate of 0.0001 and a batch size of 8 for 100 epochs. Instead of training on pixel values, SPRING was trained on a relative system of per mille (parts per thousand). This allows the network to operate using the same parameters on multiple image sizes, but restricts precision slightly.

E Evaluating Spatial Reasoning Details

E.1 GAN + CVX Baseline

Automated convex optimization is a powerful technique for solving optimization problems where the goal is to find the minimum or maximum value of a given convex function. In this method, a variety of efficient solvers are used to find the optimal solution, as long as all the constraints and the function to be optimized are convex. With recent advancements in the field, these solvers can be easily integrated into neural networks, allowing gradients to propagate through the solver seamlessly.

The GAN + CVX approach relies on this concept. In short, this method is accomplished by creating a GAN which outputs a set of parabolas – one for each positional variable – such that the neural net's "best guess" for a location is at the vertex. Then the convex optimizer finds the optimal value of the sum of parabolas subject to constraints. If a preferred value is not ruled-out by a constraint, the minimum of that variable's parabola will be selected. If it is ruled out, the result will be as close as possible to it. These constraints must be convex, which limits the library of possible constraints.

E.2 Synthetic Scenarios

In this test, we compare the performance of the spatial reasoning module alone to a generative adversarial network equipped with convex optimization as an embedded layer. We will evaluate each model's ability to meet both explicit constraints from the user and implicit preferences derived from the training data. The test scenarios will involve generating synthetic data for each object type, with the data distribution designed to express a strong preference for specific values. A range of common values for each preference will be established as acceptable, with values outside this range considered as not meeting the preference. The use of synthetic data is necessary as it allows us to know the acceptable range for each preference, which is not possible with real data. Both the spatial reasoning module and the GAN + CVX baseline will be trained on this preference-laden data, and then evaluated on their ability to satisfy constraints and preferences. The preference accuracies will be reported as the percentage of clauses that are satisfied.

The test includes three scenarios, each with specific data generation functions and acceptable preference ranges. The first scenario, "basic," involves objects with a higher likelihood of being generated on opposite halves of the image. The second scenario, "tight," has objects with specific width and height ratios with stricter acceptable ranges. The third scenario, "complex," has multiple preferences, such as object 1 being at least 1.5 times taller than its width, and object 2 having a specific y-coordinate value dependent on that of object 1. These scenarios demonstrate that the SRM's preference learning is effective and outperforms other methods such as GAN + CVX.

Two random functions were used to compose the synthetic datasets. `rnd(j, k)` randomly generates an integer between j and k from a normal distribution with mean $j + \frac{k-j}{2}$ and standard deviation $\frac{k-j}{12}$. Selected values are rounded, and constrained between j and k. For example, if object 1's *x* value is drawn from `rnd(1, 500)`, then the mean of *x* will be 250.5 and the standard deviation will be 41.583. `uni(j, k)` does the same with a uniform distribution between *j* and *k*.

The following sections include preference ranges (under "checked preferences") for each scenario. The preference accuracy is measured as a percentage of correctly satisfied clauses across 256 generated examples. The object associated with each variable is indicated in the subscript (e.g. $1 \leq x_{o1} \leq 500$ asserts that the x value of object 1 must be between 0 and 500 to satisfy the preference).

E.2.1 Basic Scenario

Object	x	y	width (w)	height (h)
1	`rnd(1,500)`	`uni(400, 550)`	`rnd(192,256)`	`rnd(128,256)`
2	`rnd(500,1000)`	`uni(400, 550)`	`rnd(192,256)`	`rnd(128,256)`

Checked preferences:

- $1 \leq x_{o1} \leq 500$
- $500 \leq x_{o2} \leq 1000$

E.2.2 Tight Scenario

Object	x	y	width (w)	height (h)
1	`rnd(1,1000)`	`rnd(300,700)`	`rnd(220,256)`	`rnd(120,150)`
2	`rnd(1,1000)`	`rnd(300,700)`	`rnd(120,150)`	`rnd(120,150)`
3	`rnd(1,1000)`	`rnd(300,700)`	`rnd(120,150)`	`rnd(220,256)`

Checked preferences:

- $220 \leq w_{o1} \leq 256$
- $120 \leq w_{o2} \leq 150$
- $120 \leq w_{o3} \leq 150$
- $120 \leq h_{o1} \leq 150$
- $120 \leq h_{o2} \leq 150$
- $220 \leq h_{o3} \leq 256$

E.2.3 Complex Scenario

Object	x	y	width (w)	height (h)
1	`rnd(1,1050)`	`rnd(375,565)`	`rnd(64, 128)`	rnd($w_{o1} \times 1.5$,200)
2	`rnd(1,1050)`	rnd($y_{o1} - 10, y_{o1} + 10$)	`rnd(64, 128)`	rnd($w_{o2} \times 1.5$,200)
3	`rnd(1,900)`	`rnd(1,144)`	`rnd(64, 128)`	rnd($w_{o3} \times 2, w_{o3} \times 2$)
4	`rnd(1,1050)`	`rnd(400,665)`	`rnd(64, 128)`	rnd($w_{o4} - 10, w_{o4} + 10$)

Checked preferences:

- $1 \leq x_{o1} \leq 1050$
- $1 \leq x_{o2} \leq 1050$
- $1 \leq x_{o3} \leq 900$
- $1 \leq x_{o4} \leq 1050$
- $375 \leq y_{o1} \leq 565$
- $y_{o1} - 10 \leq y_{o2} \leq y_{o1} + 10$
- $1 \leq y_{o3} \leq 144$
- $400 \leq y_{o4} \leq 665$
- $64 \leq w_{o1} \leq 128$
- $64 \leq w_{o2} \leq 128$
- $64 \leq w_{o3} \leq 128$
- $64 \leq w_{o4} \leq 128$
- $w_{o1} \times 1.5 \leq h_{o1} \leq 200$
- $w_{o2} \times 1.5 \leq h_{o2} \leq 200$
- $w_{o3} \times 2 \leq h_{o3} \leq w_{o3} \times 2$
- $w_{o4} - 10 \leq h_{o4} \leq w_{o4} + 10$

F Human Study Details

This section presents the details of the human study conducted to evaluate the performance of our SPRING method and Stable Diffusion inpainting for generating interior space images, such as kitchens, living rooms, and billiard rooms. We decided to conduct this study due to the difficulty of evaluating generated content for qualities like aesthetic appeal. Despite the existence of metrics like IS and FID, human studies remain the gold standard in generated image evaluation.

F.1 Study Setup

Participants were provided with a background image, a completed scene, and a bullet-pointed representation of the specification used to generate the image. Additionally, questions with images generated by SPRING displayed the intermediate layout. Background images were generated using the methods described in the main paper. Constraints were handcrafted by the authors to fit the background. This was done to produce the highest quality images possible for both algorithms, evaluating them in good conditions.

F.2 Evaluation Metrics

Participants were asked to rate each image on a 5-point Likert scale across four distinct metrics: specification satisfaction, aesthetic appeal, background preservation, and spatial naturalness.

- **Specification satisfaction:** Participants assessed how well the image adhered to the specifications, including object visibility, constraint satisfaction, and details such as color, texture, and material. The question read "On a scale of 1 to 5, how well does the image fit the prompt? This includes the objects being visible, the constraints being satisfied, and the details mentioned in the prompts (e.g. objects being the right color). Do not take image quality into account".

- **Aesthetic appeal:** Participants evaluated the overall quality of the image, regardless of its adherence to the prompt. The question read "On a scale of 1 to 5, rate the aesthetic quality of the image. This includes how realistic the image is, how good each object looks, and how good the scene as a whole looks. Do not take the prompt into account".

- **Background preservation:** Participants considered how well the original background was maintained without unnecessary alterations or damage. The question read "On a scale of 1 to 5, rate how well the background image was preserved. This includes unnecessary changes being made to the background not specified by the prompt, additional objects being added, details being unnecessarily removed, etc".

- **Spatial naturalness:** Participants assessed the proportions between objects, the proportions between an object and the background, and the natural placement of objects for their respective types. The question read "On a scale of 1 to 5, how reasonable are the locations and dimensions of the objects in the image".

F.3 Questionnaire Structure

The questionnaire included 3–4 sections, with versions 1 and 2 having three sections and version 3 having four sections. Versions were randomly assigned to each participant. Each section contained six examples generated by both SPRING and Stable Diffusion, using the same constraints and backgrounds. To ensure the validity of the responses, two attention check / gold-standard questions were incorporated into each version of the questionnaire. A total of 9 subjects, who did not violate the attention check questions, participated in the survey.

The specification satisfaction part is a multifaceted question involving some objectivity (are the positional constraints satisfied, are the right number of images displayed) and some subjectivity (do the objects look like the types they are supposed to be, do they have the right texture or material). For this reason, the specification satisfaction Likert score is preceded by two questions where the subject is asked to check the boxes for the objects that are not visible and the constraints that are not satisfied. This means the subject is forced to recognize the objective parts of specification satisfaction before taking into account the subjective ones.

F.4 Initial Tutorial

Before the test could be completed, an initial tutorial was provided to the participants. A real image was presented, and the subjects were asked to fill out the questions in the same way as they would in the main study. After completing the example, the subject was given example answers so that they could check their understanding of the directions before they began the test.

F.5 Demographics

The study included participants with diverse backgrounds to ensure a comprehensive evaluation. All subjects were college graduates with degrees in science or technology fields. Most participants had some knowledge and familiarity with generative models or AI-generated content. All subjects are currently living in the United States of America, but have diverse countries of origin. All subjects understand the English language to an advanced degree, but for some, it is a second or third language. No subjects are known to have experience in interior design. Roughly half of the subjects are currently pursuing careers in academia, while the other half are pursuing careers in industry.